Probing adsorbed polymer chains using atomic force microscopy: interpretation of rupture distributions

2004 J. Phys.: Condens. Matter 16 7199

(http://iopscience.iop.org/0953-8984/16/41/003)

INSTITUTE OF PHYSICS PUBLISHING JOURNAL OF PHYSICS: CONDENSED MATTER

J. Phys.: Condens. Matter **16** (2004) 7199–7208 PII: S0953-8984(04)76741-7

Probing adsorbed polymer chains using atomic force microscopy: interpretation of rupture distributions

Raphaël Lévy[1] **and Mounir Maaloum**[2]

Institut Charles Sadron, 6 rue Boussingault, 67083 Strasbourg Cedex, France

Received 20 February 2004, in final form 9 August 2004
Published 1 October 2004
Online at stacks.iop.org/JPhysCM/16/7199
doi:10.1088/0953-8984/16/41/003

Abstract

The conformation of adsorbed polymers is of primary importance for the properties of the generated surface. Theoretical efforts have been made to understand and predict these conformations. In several recent reports, force curves using atomic force microscopy have been proposed as a new tool to probe the conformation of adsorbed polymers through the analysis of the rupture distributions. For a dense polymer layer, many bridges form between the tip and the surface giving highly non-monotonous force profiles. Using recently developed tools for the detection of ruptures and the visualization of the rupture distributions we address the problem of the interpretation of rupture distributions. Two phenomenological constants are deduced and their physical meaning is assessed by varying experimental parameters.

(Some figures in this article are in colour only in the electronic version)

1. Introduction

Macromolecules generally interact strongly with surfaces. Even if the gain of energy per monomer is weak, once a monomer is adsorbed, there is a strong probability that other monomers will also adsorb. This energy gain must be compared to the entropy loss of the chain in order to predict its conformation (Andelman and Joanny 2000, Daoud 2000, de Gennes 1979). Polymer adsorption is used in many applications: colloid stabilization or in contrast colloid flocculation for water treatment, control of adhesive/wetting/biocompatibility of surfaces, etc. When polymer chains interact with a surface, some segments, known as trains, directly adsorb to the surface. Other segments referred to as loops stay in solution. If the end of a molecule stays in solution, then this is named a tail. The polymer conformation in the adsorbed layer governs the property of the modified surface and for this reason has motivated

[1] Present address: Biosciences Centre, Crown Street, Liverpool L69 7ZB, UK.
[2] Author to whom any correspondence should be addressed.

important theoretical efforts. However, very few experimental techniques give direct insights to the polymer conformation. Quartz crystal microbalance experiments allow the kinetics of adsorption to be measured but the measured quantities (mass and dissipation) are means on a macroscopic scale. Ellipsometry measures the thickness of the layer. Neutron or x-ray scattering give access to density profiles but cannot be performed on a regular basis. Hence there is a need for new techniques for the experimental characterization of adsorbed polymers. In the last decade, force measurements using the atomic force microscope have been proposed as a new tool to probe materials from the single molecule to the polymer layer scale. In force spectroscopy, adsorbed chain segments lead to an unravelling and stretching of the part of the molecule between the attachment points on the tip and on the surface. If several adsorption points of the chain on the surface exist, several stretching events can be observed in the force versus distance curve in the form of break off jumps. Several studies have been focused on intrinsic single molecule properties such as elasticity (Ortiz and Hadziioannou 1999, Maaloum and Courvoisier 1999) and structural transitions (Rief *et al* 1997, Oesterhelt *et al* 1999, Cluzel *et al* 1996, Hugel *et al* 2002). Interactions of polymers with solid surfaces have been probed using a polymer functionalized tip (Friedsam *et al* 2004). The first attempts to deduce polymer conformation using the force curve approach were made in 1998 by Senden *et al* on a polydimethylsiloxane/heptane/silice (Senden *et al* 1998). The same approach was used for polyacrylamide/water/mica (Senden *et al* 2000) and polyampholytes/water/gold (Ozon *et al* 2002). In these precursors studies, the loop distribution of the adsorbed polymers is identified by the rupture distance distribution. Plateaus in force curves have been observed and predicted in polyelectrolyte studies (Hugel *et al* 2002, Chatellier and Joanny 1998, Chatellier *et al* 1998). It seems reasonable to assume that the rupture distances are correlated to the size of the loops. Still, the identification of the loop size distribution with the rupture distance distribution relies on very strong assumptions. It supposes notably that the distribution of the loops is not affected by the compression of the polymer layer by the AFM tip and that the ruptures occur when the chain is completely tense, which, in favourable cases, can be checked by fitting the force profiles with a freely jointed chain model (Senden *et al* 1998). It does not take into account an eventual convolution of the distribution of the loops with the tip geometry. In a recent report, Cui *et al* have shown that it is possible to measure the loop size distribution from the distance between consecutive ruptures in an alternated copolymer (Cui *et al* 2003). However this has been demonstrated only in this specific case. It is worth noting that the rupture distribution as measured by Senden *et al* (Senden *et al* 1998) and the distance between consecutive ruptures studied by Cui *et al* (Cui *et al* 2003) are generally two different quantities. Moreover this last measurement principle relies on another hypothesis: the successive ruptures correspond to the breakage of consecutive points of attachments along the same polymer chain.

This work is focused on the interpretation of experiments where multiple bridges form between the AFM tip and the surface, which is likely to be the case for any dense polymer layer. It is sensible that the retraction curves contain relevant information about the polymer conformation and the polymer–surface interaction. However, such information is hidden in the complexity of the force profiles. Thus, the force curve analysis and the results of visualization are of primary importance. Several hundreds of curves with several ruptures in each curve have to be analysed. To address the complexity of the curves, we have chosen to focus on the rupture distributions. New ways of analysing the curves and visualizing these distributions (Lévy and Maaloum 2004) have been used to study the impact of the geometry of the AFM tip and of the cantilever stiffness on rupture distribution in a polylysine/glass/water system. Two phenomenological parameters are then deduced and by using simple models we propose an interpretation of these parameters.

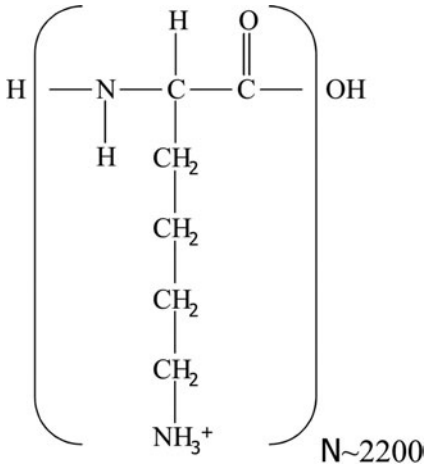

Figure 1. Polylysine.

2. Experiments and methods

Polylysine (figure 1) is a synthetic biopolymer much used in cell culture. This polymer adsorbs strongly on the glass surface and facilitates the binding and survival of cells. It is a polybase, positively charged at neutral pH since the pKa of its lateral chain is 10.2.

2.1. Force measurements

The principle of a force measurement by AFM is simple: a surface is repeatedly extended towards and retracted away from a sharp tip (fixed to a cantilever) and the position of the tip is recorded as a function of the surface displacement. To achieve accurate quantitative results, it is imperative to measure as precisely as possible the spring constant of the cantilever. The thermal fluctuation method has been shown to be a good method when the shape of the mode and the repartition of the energy between the vibration modes are taken into account (Lévy and Maaloum 2002, Butt and Jaschke 1995). The spring constant of the cantilevers used in our experiments is equal to 10 ± 2, 32 ± 3 and 96 ± 10 mN m^{-1}.

We have developed a program which allows us to automatically detect the ruptures. The algorithm is based on an analysis of the standard deviation in a sliding window along the length of the force curve (Lévy and Maaloum 2004). Automatic detection of ruptures constitutes an important step forward because the time required to analyse the curves is significantly reduced, thus allowing the user to perform multiple experiments. In addition the automatic analysis eliminates the bias related to the subjective choice of a manual analysis.

In a force curve, a rupture R_i is characterized by two parameters selected among the three following magnitudes: surface displacement (D_i), tip–surface separation (S_i) and cantilever deflection (d_i). The surface displacement is set to a value of zero at the intersection of the baseline ($d = 0$) and the compliance line ($S = 0$). As can be deduced from figure 2, the three parameters are linked by the following equation: $D_i = S_i + d_i$. In this work, the retraction speed is kept constant (50 nm s^{-1}). As a consequence, the surface displacement D is also proportional to the duration of applied force. The rupture distributions are presented in the form of a density map in a plane where both axes correspond to the selected parameters. The main advantage of this kind of representation is that it allows the investigation of the whole ruptures and the correlation between force and distance in a single graph.

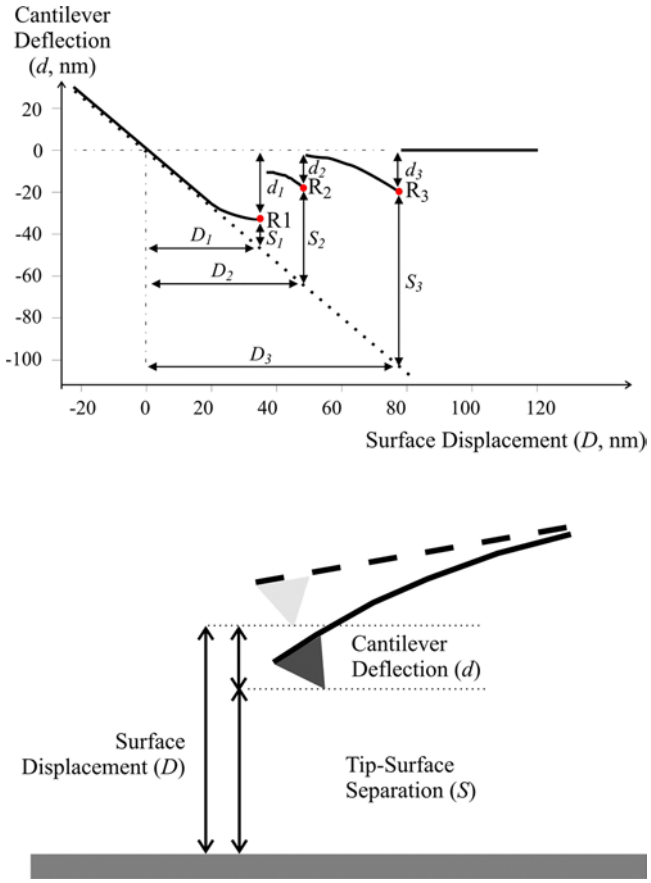

Figure 2. Cantilever deflection during the retraction of a surface from an AFM tip. *Top*: curve showing three rupture events $R_1(d_1, D_1, S_1)$, $R_2(d_2, D_2, S_2)$, $R_3(d_3, D_3, S_3)$. The surface displacement is set to a value of zero at the intersection of the baseline ($d = 0$) and the compliance line ($S = 0$). The force can be obtained by multiplying the deflection S by the spring constant of the cantilever. *Bottom*: Scheme showing the relation between the three parameters d, D and S.

3. Results and discussions

3.1. Adsorption

Polylysine (M_W 200 000–300 000, *Sigma*) adheres strongly to unmodified AFM tips. This adhesion is demonstrated by numerous events detected in the force curves between the unmodified tip and a layer of polylysine adsorbed on a glass surface (figure 3). The distribution of the distances between adjacent ruptures (S_{i+1}–S_i) is characterized by a maximum l_{max} followed by an exponential decay with a characteristic length l_{dec} (figure 4). Similar distance distributions have been observed for other polymeric systems, such as statistical copolymers and homopolymers (PNIPAM) (Haupt *et al* 2002), polyampholytes (Ozon *et al* 2002) and alternated copolymers (Lévy 2002). What is the physical significance of these two lengths, as well as the origin of this law?

To answer this question and more generally to achieve a better understanding of force spectroscopy results on a polymer layer, experimental parameters (tip geometry and cantilever stiffness) have been varied and their influence on rupture distributions is discussed.

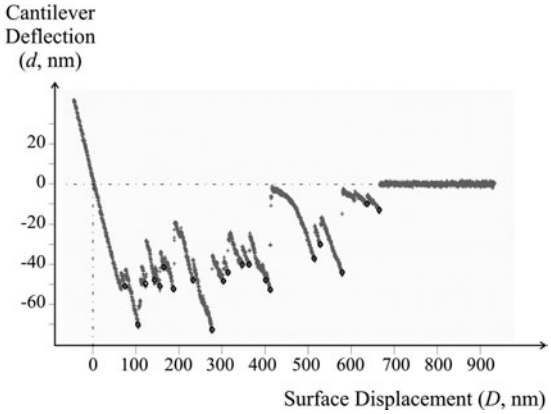

Figure 3. Force curve between adsorbed poly-L-lysine on glass in water. The black circles highlight the detected ruptures.

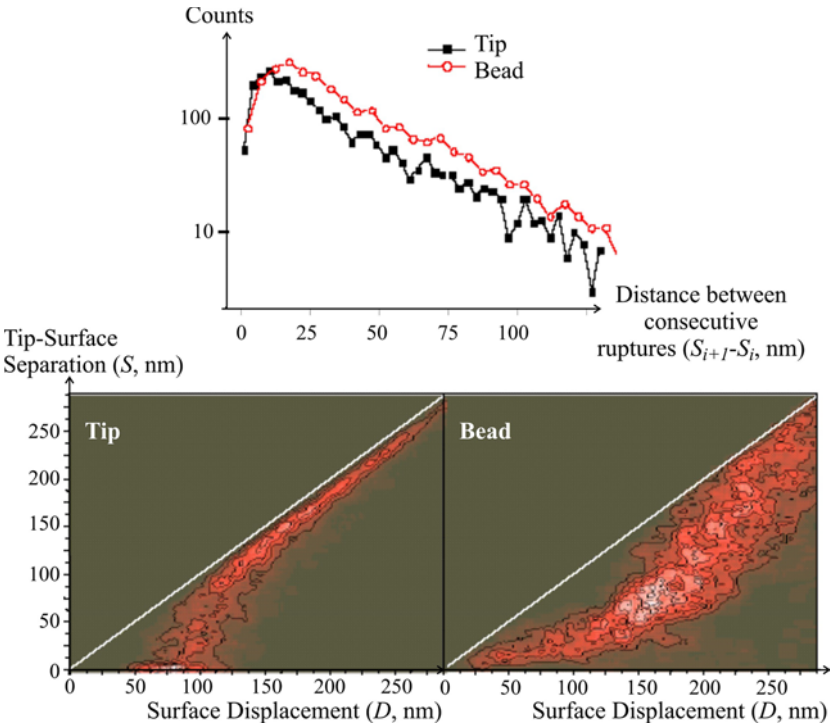

Figure 4. Rupture distributions for force measurements done with an unmodified tip and with a glass bead (radius$\sim$15 μm) glued on the tip. *Top*: histogram of distances between consecutive ruptures S_{i+1}–S_i. *Bottom*: rupture distributions in the (S, D) plan.

3.2. Effects of AFM tip geometry

To vary the contact geometry, a glass bead was attached to the AFM tip. The stiffness and rheological properties of the cantilever are not significantly affected (data not shown) because the size of the bead is of the same order of magnitude as the tip height and much smaller than the cantilever width and length. But the radius of curvature of the probe is radically changed from

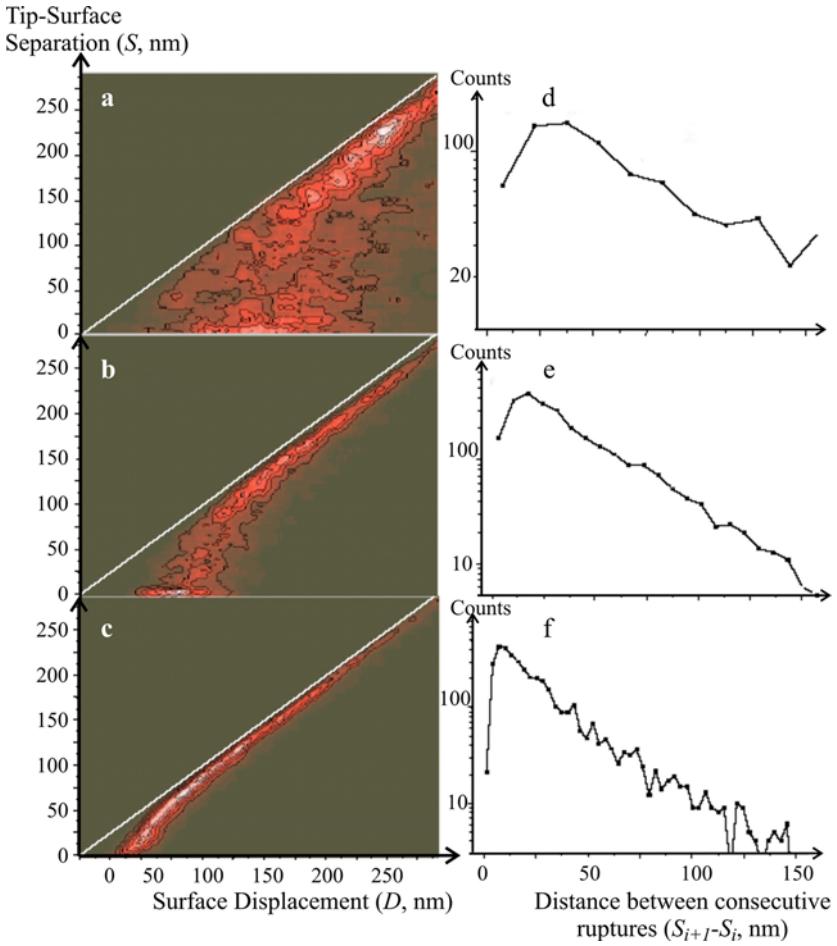

Figure 5. Rupture distributions for force measurements done with probes of different stiffness on the same polymer layer. *Left*: Rupture distributions in the (S, D) plan for cantilevers of 10 mN m^{-1} (a), 32 mN m^{-1} (b) and 96 mN m^{-1} (c). *Right*: Histogram of distances between consecutive ruptures S_{i+1}–S_i for cantilevers of 10 mN m^{-1} (d), 32 mN m^{-1} (e) and 96 mN m^{-1} (f).

approximately 50 nm to 15 μm. As can be seen in figure 4 the rupture distribution is profoundly modified. The number of ruptures per curve was not significantly modified (data not shown), but the ruptures occurred later and for stronger forces (figure 4, bottom). Surprisingly, we find the same value of 35 nm for the decay length l_{dec} in these two experiments performed on the same polymer layer, either with an AFM tip or with a glass bead (figure 4 top). However the maximum of the distribution is significantly shifted: l_{max} increases from 9 to 17 nm.

3.3. Effects of the cantilever spring constant

The effect of change in cantilever stiffness on the decay length and on the rupture distribution is shown in figure 5. The spring constant varies from 10 to 32 then 96 mN m^{-1}. This experiment demonstrates a reduction of the lengths l_{max} and l_{dec} when the stiffness of the cantilever is increased (figures 5(d)–(f)). l_{max} decreases from 33 to 16 and then 9 nm, whereas l_{dec} decreases from 65 to 35 and then 23 nm. The distribution of the ruptures in the displacement/separation

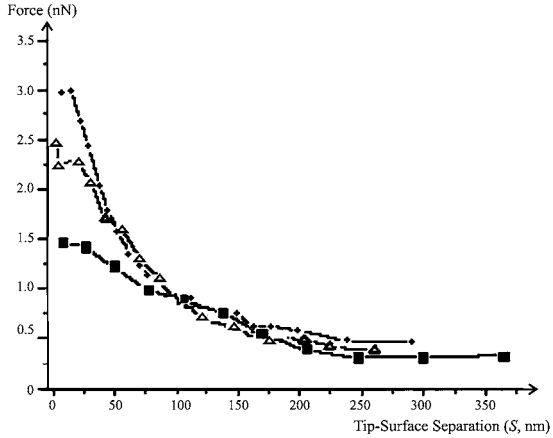

Figure 6. Mean rupture force for measurements done with cantilevers of 10 mN m^{-1} (black squares), 32 mN m^{-1} (hollow triangles) and 96 mN m^{-1} (crosses).

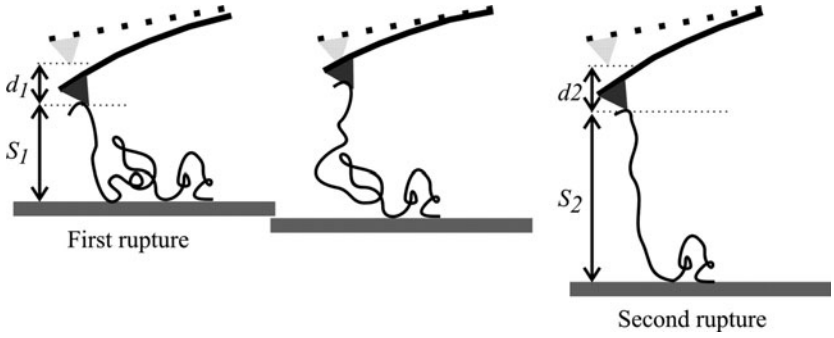

Figure 7. Schematic of polymer pulling.

plane is greatly modified (figures 5(a)–(c)). The ruptures occur after longer displacements and at larger tip–surface separations with a soft spring than with a stiff spring.

The presentation using a density map in the displacement/separation plane does not allow an easy determination of the force variation as a function of the stiffness. Figure 6 shows a decrease of the mean force as a function of the separation for the three cantilevers. The mean force for short separations increases with the spring constant of the cantilever. For large range separations, the mean force depends only weakly on the spring stiffness.

3.4. Correlation between successive ruptures

In the simple model of chain extension shown in figure 7, the distance between successive ruptures (S_{i+1}–S_i) corresponds to the size of a loop. This simple model assumes that successive ruptures correspond to the breakage of consecutive points of attachment along the polymer chain (Cui *et al* 2003). In a sense, the ruptures are then correlated through the existence of the loop. Another extremely simple model would be to assume that at the moment of contact, a certain number of bridges of different sizes are formed between the tip and the surface, and are then broken during extension. In this latter case, the distribution of the distances between ruptures is a simple result of the distribution of the sizes of the bridges formed initially: the successive ruptures are not correlated.

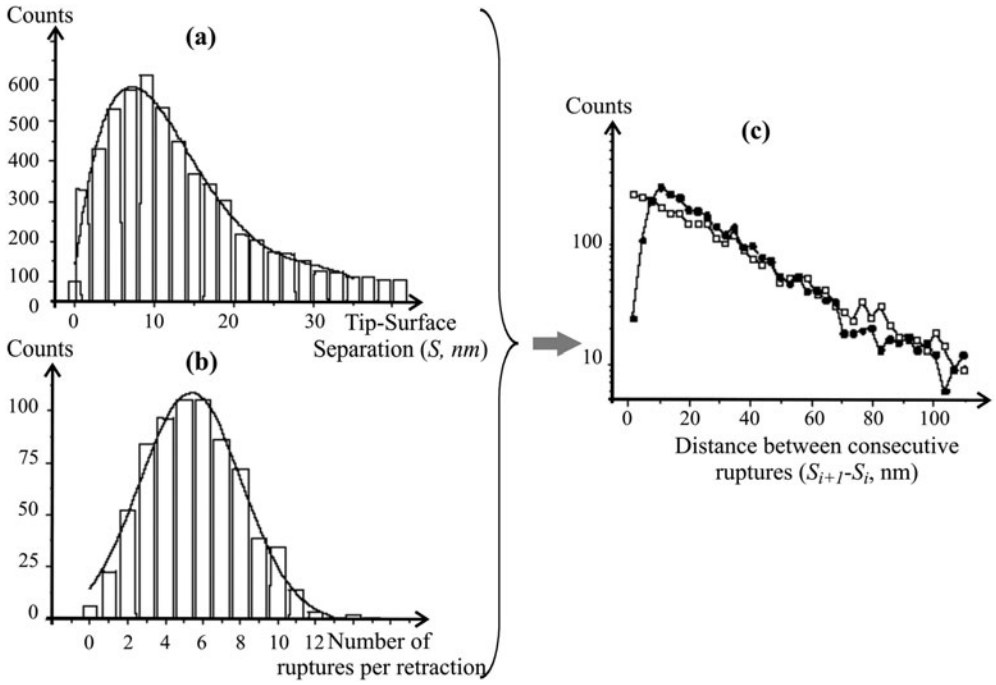

Figure 8. Correlation between consecutive ruptures. Histograms of tip–surface separations S_i (a) and of the number of ruptures per approach–retraction cycle (b). From these two histograms, a distribution of distances between consecutive ruptures was generated ((c), empty symbols) and compared to the experimental one ((c), full symbols).

It is clear that these models cannot take into account the complexity of the results presented in the previous paragraphs. Nevertheless, the question of whether or not the successive ruptures are correlated remains and has a large impact on the interpretation of experiments. One way of reformulating this question, in direct relation to the experimental results, is to ask whether the distribution of the distances between ruptures (S_{i+1}–S_i) can be inferred from the distribution of the rupture distances (S_i) and the distribution of the number of ruptures per approach–retraction cycle. In other words, does the succession of ruptures in each force curve contain more information than the average rupture probability?

In order to answer this question, rupture distances were numerically generated according to a probability law deduced from an experiment (figure 8(a)). These distances were then clustered into small groups to simulate the force curves. The number of ruptures in each group was chosen using the distribution of the number of ruptures per approach–retraction cycle from the same experiment as a probability law (figure 8(b)). Figure 8(c) compares the distributions of the distances between ruptures deduced from this simulation with those deduced from the experimental results[3]. In both cases we obtain an identical exponential decrease.

[3] The simulation is proportional to an autocorrelation function of a rupture probability law, or more precisely to a pondered sum of autocorrelation functions corresponding to the different class of curves defined by the number of ruptures per curve. In figure 8(c), the difference between the simulation (empty symbols, no maximum) and the 'experimental' (full symbols, maximum) come from the following fundamental difference. In the 'simulation', the curve results from the autocorrelation of a probability law, whereas in the 'experiment' the curve results from the autocorrelation of the ruptures observed in each individual force curve.

3.5. Interpretation of rupture distributions

The simulation described in the previous section permits an interpretation of the lengths l_{max} and l_{dec}. The exponential decay length l_{dec} can be deduced from the rupture distributions and the number of ruptures per curve (figure 8). Therefore l_{dec} is not related to any correlation between consecutive ruptures and is not directly related to the loop size distribution. l_{dec} measures the width of the rupture distances distribution and the mean number of ruptures per curve (the more the ruptures are spread, the larger l_{dec} will be; the larger the number of ruptures per curve, the smaller l_{dec}).

The simulated distribution has no maximum. The maximum in the experimental distributions is due to a smaller number of events separated by short distances than predicted by the simulation. As the simulation corresponds to the absence of correlation, we can assume that l_{max} is an anticorrelation length; when a rupture occurs, it is unlikely that another rupture occurs before l_{max} (Al-Maawali *et al* 2001).

This interpretation of l_{max} is supported by the analysis of the results as a function of the stiffness of the spring. l_{max} increases when the spring stiffness is reduced. The amplitude of the cantilever relaxation after a rupture R_i will be larger for a soft spring than for a stiff spring. For similar rupture forces and full relaxation (the cantilever returns to equilibrium), this is simply due to the Hook law. If the relaxation is complete, the amplitude is equal to the cantilever deflection at the rupture. If the relaxation is incomplete, the relaxation is smaller than this deflection. On average, the deflections and hence the relaxations, are larger for soft springs than for stiff springs. When a rupture occurs, the tip–surface separation is suddenly increased by the amplitude of the cantilever relaxation. As long as the molecular bridge between the tip and the surface is not an 'active bridge' capable of reducing the tip–surface separation, the tip–surface separation will continue to increase until the next rupture occurs. Thus, the next rupture R_{i+1} will occur at a distance superior to this relaxation distance: $S_{i+1}-S_i > relaxation_i$ and a larger anticorrelation length is expected for softer springs.

Similarly, when the tip radius is increased the tip–surface interaction energy will be greater leading to a greater relaxation and hence to a larger value of l_{max} in qualitative agreement with our experimental data.

As seen previously, the effect of a change in the stiffness of the spring is not limited to this variation of the anticorrelation length l_{max}. The distribution of the ruptures is significantly modified (figures 5 and 6). We propose therefore a model in which a reorganization of the links occurs during the retraction. With a stiff spring, during the retraction, the tip rapidly leaves the polymer layer. In contrast, with a soft spring the force slowly increases and the bridges between the tip and the surface are reorganized, giving rise to longer bridges. This reorganization is driven by the balance between the adsorption energy and the stretching energy of the polymer.

4. Conclusion

We have performed a set of experiments consisting of stretching adsorbed polymers using the AFM tip. We have demonstrated a length of anticorrelation between successive ruptures that depends on the stiffness of the cantilever. The spectacular effect of the change of spring stiffness on the separations at which ruptures occur shows that it is necessary to take into account the dynamics of the polymer as well as the geometry and stiffness of the probe in the interpretation of these experiments, especially in the case where multiple bridges link the tip and the surface. Depending on the experimental parameters, stretching adsorbed polymers can probe the conformation of the chains (situation out of equilibrium in which the elasticity of the

chains predominates but no reorganization occurs) or probe an adsorption energy (Portigliatti *et al* 2000). A complete understanding of this transition will require additional experiments with systematic variations of the separation velocities, contact times and applied loads.

References

Al-Maawali S, Bemis J E, Akhremitchev B B, Leecharoen R R, Janesko B G and Walker G C 2001 *J. Phys. Chem.* B **105** 3965–71

Andelman D and Joanny J-F 2000 *C. R. Acad. Sci.* IV **1** 1153–62

Butt H-J and Jaschke M 1995 *Nanotechnology* **6** 1

Chatellier X and Joanny J F 1998 *Phys. Rev.* E **57** 6923–35

Chatellier X, Senden T J, Joanny J F and di Meglio J M 1998 *Europhys. Lett.* **41** 303–8

Cluzel P, Lebrun A, Heller C, Lavery R, Viovy J L, Chatenay D and Caron F 1996 *Science* **271** 792–4

Cui S X, Liu C J, Zhang W, Zhang X and Wu C 2003 *Macromolecules* **36** 3779–82

Daoud M 2000 *C. R. Acad. Sci.* IV **1** 1125–33

de Gennes P-G 1979 *Scaling Concepts in Polymer Physics* (Ithaca, NY: Cornell University Press)

Friedsam C, Becares A D, Jonas U, Gaub H F and Seitz M 2004 *Chem. Phys. Chem.* **5** 388–93

Haupt B J, Senden T J and Sevick E M 2002 *Langmuir* **18** 2174–82

Hugel T, Holland N B, Cattani A, Moroder L, Seitz M and Gaub H E 2002 *Science* **296** 1103–6

Lévy R 2002 *PhD Thesis* Université Louis Pasteur, Strasbourg
http://tel.ccsd.cnrs.fr/documents/archives0/00/00/15/65/tel-00001565-02/index.htm

Lévy R and Maaloum M 2002 *Nanotechnology* **13** 33–7

Lévy R and Maaloum M 2004 *Ultramicroscopy* at press

Maaloum M and Courvoisier A 1999 *Macromolecules* **32** 4989–92

Oesterhelt F, Rief M and Gaub H E 1999 *New J. Phys.* **1** 6.1–11

Ortiz C and Hadziioannou G 1999 *Macromolecules* **32** 780–7

Ozon F, di Meglio J M and Joanny J F 2002 *Eur. Phys. J.* E **8** 321–30

Portigliatti M, Hervet H and Leger L 2000 *C. R. Acad. Sci.* IV **1** 1187–96

Rief M, Oesterhelt F, Heymann B and Gaub H 1997 *Science* **275** 1295–7

Senden T J, di Meglio J M and Auroy P 1998 *Eur. Phys. J.* B **3** 211–6

Senden T J, di Meglio J M and Silberzan I 2000 *C. R. Acad. Sci.* IV **1** 1143–52